Analysis of Hydrogen Combustion in a Spark Ignition Research Engine with a Barrier Discharge Igniter

Federico Ricci , Massimiliano Avana , Jacopo Zembi , Carlo Nazareno Grimaldi , Michele Battistoni * , Stefano Papi

Posted Date: 4 March 2024

doi: 10.20944/preprints202403.0144.v1

Keywords: Hydrogen fuel; SI engine; Barrier Discharge Igniter; ultra-lean combustion

Article

Analysis of Hydrogen Combustion in a Spark Ignition Research Engine with a Barrier Discharge Igniter

Federico Ricci [1], Massimiliano Avana [1], Jacopo Zembi [1], Carlo Nazareno Grimaldi [1], Michele Battistoni [1,*] and Stefano Papi [2]

[1] University of Perugia, Department of Engineering, Via G.Duranti 93 06125 Perugia PG
[2] Federal-Mogul Powertrain Italy, Via della Scienza, 6/8, 41012 Carpi MO
* Correspondence: michele.battistoni@unipg.it

Abstract: Hydrogen fuel is gaining particular attention in internal combustion engines. In addition to zero-carbon emissions, major advantages relate to its combustion characteristics, which allow significant increase in thermal efficiency under ultra-lean operation and with very low NOx levels. The ignition system is one of the main technology enablers, as it determines the capability to control ultra-lean operations, avoid backfire phenomena, or reduce the risks of abnormal combustions. The latter results from the hydrogen low ignition energy and it is associated with factors like high-temperature residuals, hot spots, and irregular spark plug discharge. ACIS gen 2-Barrier Discharge Igniter excels in accelerating the initial flame growth speed by the generation of non-equilibrium low-temperature plasma, strong ignition promoter for the combined action of kinetic and thermal effects. Moreover, its volumetric discharge facilitates combustion initiation on a wide region, in contrast to the localized ignition of traditional spark systems. In this work we present for the first time, to the best of our knowledge, experimental results showing the performance of a hydrogen engine with a low-temperature plasma discharge. Tests were conducted on a single-cylinder research engine, achieving ultra-lean conditions with cycle-to-cycle variability results below 2.5%. The analysis indicates that the H2 - BDI combined solution is capable of accelerating the evolution of the flame front compared to traditional spark plugs, leading to a significant reduction in the cycle-to-cycle variability. A meticulous adjustment of the BDI control parameters further enhances igniter performance and contributes to a deeper understanding of the innovative approach proposed in this study.

Keywords: hydrogen fuel; SI engine; barrier discharge igniter; ultra-lean combustion

1. Introduction

In response to the imperative to reduce carbon emissions in the transportation sector and address air quality concerns, regulations related to pollutant emissions and greenhouse gases are driving the development of cleaner and more efficient internal combustion engines (ICE) [1]. Advanced after-treatment systems, such as high-efficiency particulate filters (D/GPF), selective catalytic reducers (SCRs) with urea injection, and modern catalyst light-off strategies, are effectively minimizing pollutant emissions (NOx, CO, unburned hydrocarbons, and particulate matter) to nearly zero [2]. Traditional spark ignition (SI) engines face challenges in ensuring high performance together with low emissions [3]. In the context of modern spark ignition (SI) engines, the approach to reducing fuel consumption involves implementing high boost levels in conjunction with downsizing [4], along with the adoption of water injection [5,6], lean and/or Exhaust Gas Recirculation (EGR) diluted mixtures [7,8]. It is crucial to explore contemporary combustion strategies like low-temperature combustions (LTCs) [9], increase the hybridization level of vehicles to meet the requirements of sustainable mobility [10] and promote the use of renewable and alternative fuels [11].

 doi:10.20944/preprints202403.0144.v1

In this contest, hydrogen H_2 is recognized as the energy vector guiding towards a fossil fuel-free future of mobility, since it stands out as the only fuel with the potential to eliminate carbon, carbon monoxide, and carbon dioxide emissions, allowing for high efficiencies under very lean combustion conditions [12]. The wide flammability limits and rapid flame propagation rate of hydrogen contribute to a stable combustion process, particularly for lean mixtures [13]. Hydrogen can be employed in an internal combustion engine in various modes, including dedicated fuel operation as well as in bi-fuel or dual-fuel configurations. Numerous studies have been conducted to promote the use of hydrogen fuel in internal combustion engines [14], whether as a sole fuel or by adding it to fossil fuels to enhance engine brake thermal efficiency and reduce exhaust emissions [15]. Due to the highly dilute mixtures and the elevated autoignition temperature, hydrogen engines can withstand higher compression ratios (up to 14.5:1) compared to gasoline engines [16]. This characteristic results in enhanced thermodynamic efficiency [17]. Consequently, the engine can operate with load quality regulation, eliminating the need for a throttle, potentially achieving an engine efficiency of 52% [18]. As found by Shi et al. [19], the brake thermal efficiency witnessed an increase from around 10.0% to 16.7% under an excess air ratio of 1.3, when 6% of hydrogen is added to gasoline of a retrofitted Wankel engine. Dimitriou et al. [20] demonstrated an enhancement in brake thermal efficiency, with the maximum improvement reaching approximately 3%, correlating to an 80% addition of hydrogen energy. When pure hydrogen is utilized, HC and CO concentrations approach zero, with only minimal contributions from lubricating oil combustion [21]. Serin et al. [22] also showcased reductions in CO emissions through hydrogen additions, albeit accompanied by an increase in NOx emissions. Despite the mentioned benefits, the use of hydrogen in ICEs presents challenges, particularly in addressing abnormal combustion issues, issues, both as an in-cylinder process or as backfire in port fuel injection (PFI) engines [23]. The occurrence of backfire, an abnormal combustion in PFI engines, hinders further advancements in engine performance. This is due to factors such as low ignition energy and high flame propagation velocity [24]. When backfire happens, the volumetric efficiency of port fuel injection engines significantly decreases, leading to power loss [25]. Backfire can also trigger engine knock [26], causing damage to cylinders and pistons [27]. Moreover, the intake systems and hydrogen injectors may suffer damage from high temperatures resulting from hydrogen combustion in the intake manifold [28]. Consequently, less hydrogen is delivered into the cylinders. Backfire in port fuel injection engines is typically caused by high residual exhaust gas temperature, hot spots, and abnormal ignition [29], all of which heavily depend on the engine's operating conditions. To mitigate these challenges, preventing pre-ignition due to hot spots around the spark plug and reducing ghost spark phenomena related to standard ignition coils is crucial. As reported in [30], this can be achieved through the adoption of a cooled ignition system or unconventional ignition methods, like corona discharge, which not only prevents pre-ignition and backfire but also facilitates the ignition of highly diluted hydrogen-air mixtures [23].

1.1. Present Contribution

Within this contest, the present work presents, for the first time to the best of our knowledge, experimental results showing the performance of a hydrogen engine with a low-temperature plasma (LTP) discharge, namely Advanced Corona Ignition System of second generation Barrier Discharge Igniter (ACIS gen2-BDI) [31,32]. By generating ionization waves through the corona effect, BDI stands out in enhancing the initial flame growth speed. This is achieved through the creation of non-equilibrium low-temperature plasma, acting as a potent ignition promoter by combining kinetic and thermal effects [33,34]. Additionally, the BDI volumetric discharge allows for combustion initiation across a broad region, contrasting with the localized ignition typical of traditional spark systems [35]. Results from the same research group demonstrated the capability of BDI to extend the lean stable limit if compared to traditional spark when operating with fuels like gasoline E5 and ethanol E85 [36]. Moreover, the lack of a prominent ground electrode in the BDI system serves to minimize heat losses and eliminates hot-points susceptible to pre-ignition. Additionally, the power electrode remains indirectly exposed to the effects of excited species generated during the discharge [37]. Using a single cylinder research engine operating at 1000 rpm and in low-load conditions (IMEP = 4.5 bar

 doi:10.20944/preprints202403.0144.v1

at λ = 1.0 when operating with spark-E5 [38]), a first experimental campaign was conducted. By means of indicating analysis, a comparison between the performance of ACIS gen 2-BDI and conventional spark plug was conducted in H_2 in order to assess the differences in terms of control, combustion behavior, and the ability to extend the lean stable limit of the engine. Tests were carried out starting from a λ value of 1.6, which corresponds to the lean limit achieved with spark-E5 [36]. By controlling hydrogen flow rate, the experiments extended up to leaner condition where the Indicated Mean Effective Pressure (IMEP) was lower by less than 1 bar compared to the maximum values achieved in the engine using a spark-E5 configuration. The results show the ACIS gen 2-BDI system's capacity to accelerate the flame front propagation, evident through altered in-cylinder pressure patterns and enhanced stability at optimized ignition timings. At λ = 1.6, hydrogen displayed lower IMEP if compared to gasoline E5 application but superior combustion stability with a reduced cycle-to-cycle variability. Hydrogen's lower ignition timing requirement stemmed from its combustion traits, including higher flame speed and wider flammability range. Moreover, when compared to traditional spark ignition, the ACIS gen 2-BDI system showcased an ability to advance combustion, extending the lean stable limit, without backfire events due to its heat-loss minimizing design and residual energy storage reduction. Investigating leaner conditions (λ = 2.0 and λ = 2.3) emphasized the necessity for advanced ignition timing to center combustion within the Maximum Brake Torque (MBT), where despite reduced maximum in-cylinder pressure and IMEP, the ACIS gen 2-BDI system demonstrated stability with a less pronounced reduction in CoV_{IMEP}, underlining hydrogen's broader flammability range. In essence, the ACIS gen 2-BDI system displayed promising capabilities in enhancing combustion characteristics and stability, thereby accentuating its potential for efficient and stable operation in lean conditions with hydrogen fuel. The evaluation suggests that the integration of H_2 with the ACIS gen 2-BDI system has the capability to expedite the progression of the flame front when compared to conventional spark plugs. This results in a notable decrease in the variability observed from one engine cycle to the next. Through a careful fine-tuning of the ACIS gen 2-BDI control parameters, the performance of the igniter is further improved, offering insights into the innovative approach presented in this study.

2. Materials and Methods

2.1. Igniter

An ACIS second-generation BDI prototype has been selected as igniter, synthetically identified as ACIS gen2-BDI, supplied by Federal Mogul Powertrain Italy, a Tenneco Group Company, which is capable to generate a robust electric field within the combustion chamber at a frequency of approximately 100 kHz. This device is referred to as ACIS gen2-BDI to distinguish it from a previously studied prototype by the same research group, which operates at an input frequency of around 1.04 MHz [36,38]. The streamers produced by ACIS gen2-BDI start from the annular grounded electrode, located along the base circumference of the igniter, and propagate on the surface of the dielectric material that covers the counter-electrode. The corona igniter, as depicted in Figure 1, can directly receive power from the engine battery and trigger signals from the engine control unit. To enhance control over the voltage supplied to ACIS gen2-BDI during tests, an external power supply has been utilized. Specialized software facilitates the adjustment of control parameters for device ignition, including the driving voltage (V_d) and activation time (t_{on}). These parameters are respectively associated with the peak electrode voltage reached at the igniter's firing end and the discharge duration of the device [32]. From now on, ACIS gen2-BDI will be referred as BDI for the sake of simplicity.

Preprints.org (www.preprints.org) | NOT PEER-REVIEWED | Posted: 4 March 2024 doi:10.20944/preprints202403.0144.v1

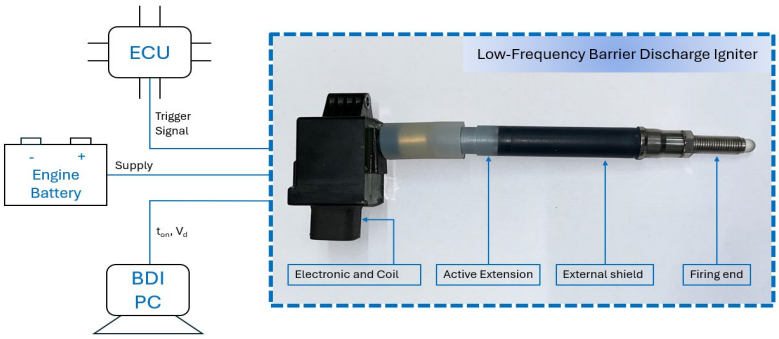

Figure 1. Operating configuration and characteristics of the ACIS gen2-BDI prototype.

2.2. Single Cylinder Research Engine

Measurements were carried out on a 500-cc single-cylinder engine (Figure 2a) with four valves, pent-roof combustion chamber, and a reverse tumble intake port system which is designed to operate in Direct Injection (DI) or PFI modes. Further details are reported in Table 1. The tests were conducted at 1000 rpm in PFI mode with the igniters centrally located (Figure 2b). The engine can be also configurated to allow optical access, however, in this work the quartz piston crown was replaced by a metal one (Figure 2c). The optical configuration requires dry contact [38] between cylinder liner and piston rings, so that the latter are realized in a Teflon-graphite mix. For all other moving parts of the engine, a conventional mineral lubricant was used: its temperature, together with the coolant one, was set at 343.0 ± 0.2 K. This value was chosen to guarantee longer engine durability and a reduced blow-by. Piston thermal expansion was close to the tolerance limit and piston crown temperature was in the expected range of SI applications, even if coolant is about 20 K lower than commercial power units [38].

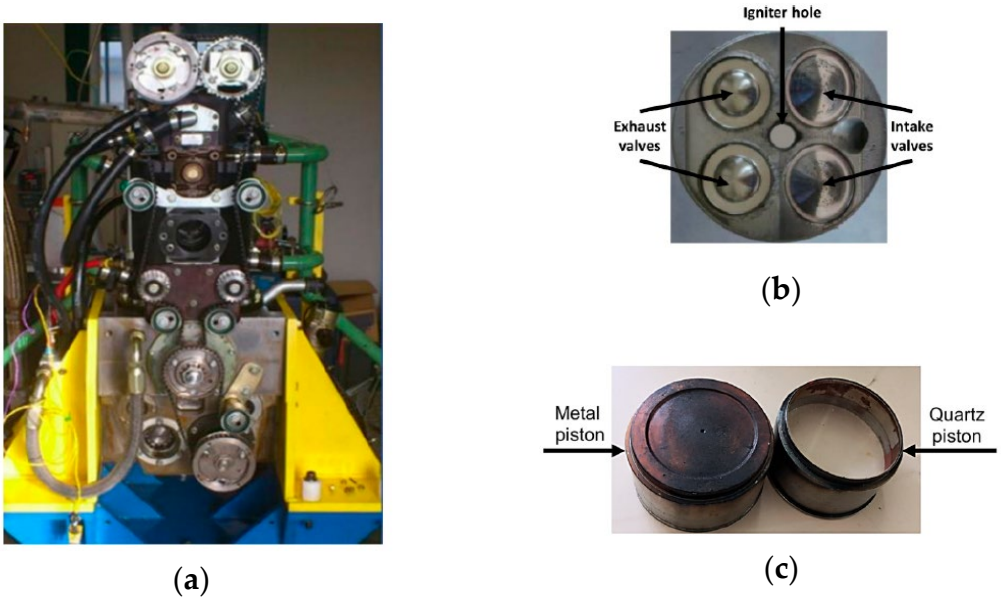

Figure 2. (a) test engine, (b) details of engine head, (c) metal piston (left) and quartz one (right).

Table 1. Engine data.

Feature	Value	Unit
Displaced volume	500	cc
Stroke	88	mm
Bore	85	mm
Connecting rod length	139	mm
Compression ratio	8.8:1	-

Preprints.org (www.preprints.org) | NOT PEER-REVIEWED | Posted: 4 March 2024 doi:10.20944/preprints202403.0144.v1

Number of valves	4	-
Exhaust valve open	-13	CAD aBDC
Exhaust valve close	25	CAD aBDC
Intake valve open	-20	CAD aBDC
Intake valve close	-24	CAD aBDC

Air-flow rate was set by means of a throttle valve upstream of the intake manifold; its position was maintained fixed for all the test points, so that the air-flow towards the combustion chamber, as well as the in-cylinder charge motion, did not change. Air-fuel ratio was controlled only by increasing or decreasing the hydrogen fuel injected quantity, which is injected at fixed injection pressure of 4 bar absolute. A research ECU (Athena GET HPUH4) controlled the energizing time of the injector and the ignition timing (IT) by sending a trigger signal to the igniter control unit. A piezoresistive transducer (Kistler 4075A5) on the intake port measured the intake pressure and a piezoelectric transducer (Kistler 6061 B) on the side of the chamber measured the in-cylinder pressure. A Kistler Kibox combustion analysis system (Figure 3), with a temporal resolution of 0.1 CAD, acquired the pressure signals, the absolute crank angular position measured by an optical encoder (AVL 365C), the O_2% was measured by a fast probe at the exhaust (Horiba MEXA-720, accuracy of ±2.5%). The ignition signal from the ECU was also acquired by the indicating system. A total of 103 consecutive combustion events were recorded for each operating point tested.

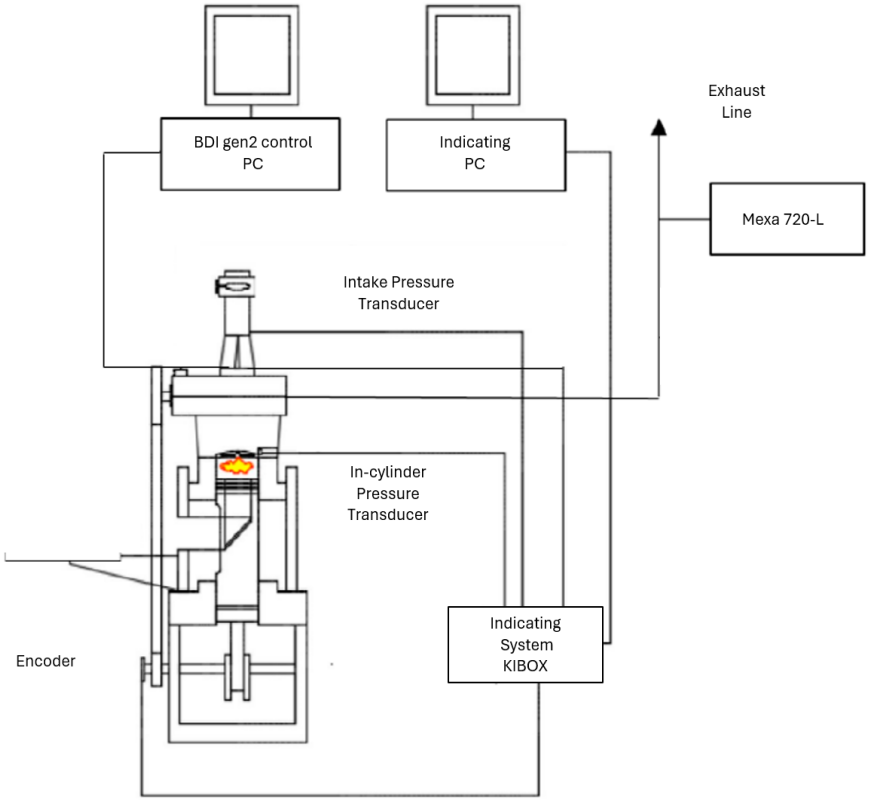

Figure 3. Test engine setup.

During engine operation, the λ value is adjusted in real-time towards the desidered value based on the O_2% concentration, using the formula proposed by Azeem et al. [39] (Equation (1)):

$$\lambda = \frac{1 + Xo2}{1 - \frac{Xo2}{Yo2}} \quad (1)$$

where $Xo2$ and $Yo2$ are the wet concentrations of oxygen in the exhaust gas and intake air respectively.

 doi:10.20944/preprints202403.0144.v1

2.3. Test Campaign

The experimental campaign is based on the examination of BDI's performace at lean conditions on a conventional PFI engine using hydrogen H_2 at low speed (1000 rpm) and low load.

The primary stage consists on the investigation carried out on the BDI's control parameters at λ = 1.6. By setting the activation time to t_{on} = 2 ms, we first optimized the combination with V_d = 11 V in terms of ignition timing to determine the MBT. Following that, we carried out the same optimization process, this time considering V_d = 12.5 V.

Subsequently, the aim is to conduct a comparative analysis, under the same operating conditions (λ = 1.6), evaluating the performance achieved with the ignition of both gasoline E5 and hydrogen H_2 using BDI system. This assessment will encompass a comprehensive examination of various parameters, including Indicating Data (AI05, AI50, AI90, IMEP and CoV_{IMEP}), in-cylinder pressure and IHRR (Integral Heat Release Rate), considering the ignition timing optimized for each scenario.

Furthermore, it is made a comparison beetween the traditional spark igniter and the BDI to discern the propensity for back-firing induced by the utilization of the traditional ignition system in conjuction with hydrogen as the fuel source.

In the conclusive step of this investigation, under the optimized operating conditions of the BDI system, the air-hydrogen mixture is progressively leaned out up, from λ =1.6 to λ = 2.3. With the porpouse of achieving a more optimal and stable combustion process, considering the Indicating Data, in-cylinder pressure and IHRR, by centering half of the combustion within the MBT area, the IT has to be advanced moving towards leaner conditions because of the combustion duration increment.

3. Results and Discussions

3.1. Optimization of the BDI Performance at λ = 1.6

Figure 4 shows the results of the investigation carried out on the BDI's control parameters at λ = 1.6. By fixing the activation time to t_{on} = 2 ms, first, the combination presenting V_d = 11 V has been optimized in terms of ignition timing in order to determine the MBT. After that, the same optimization process has also been realized by considering V_d = 12.5 V.

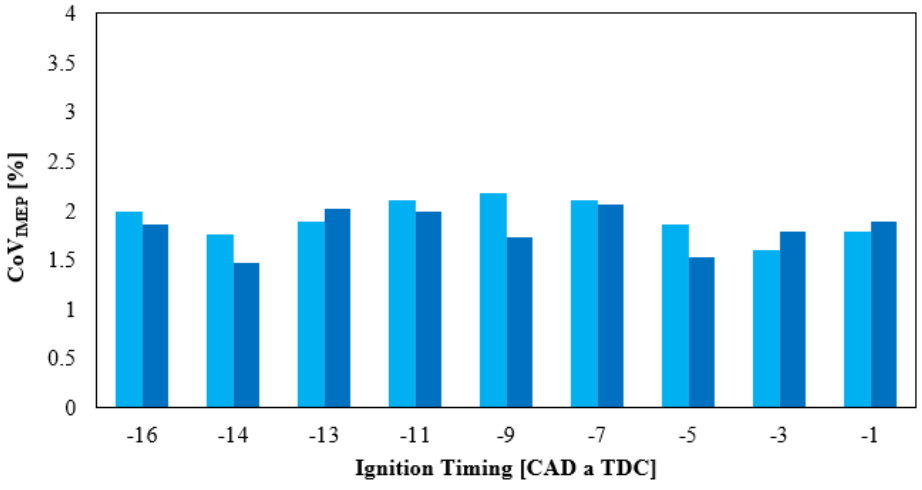

(a)

 doi:10.20944/preprints202403.0144.v1

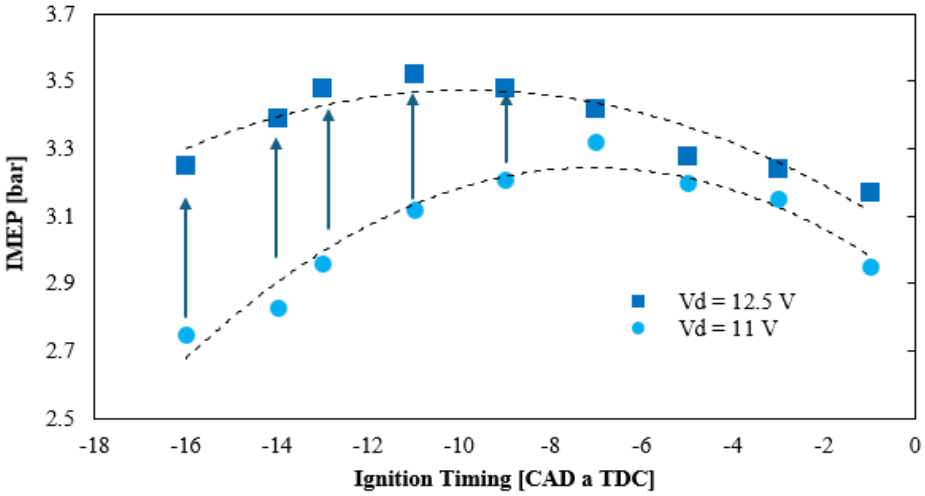

(b)

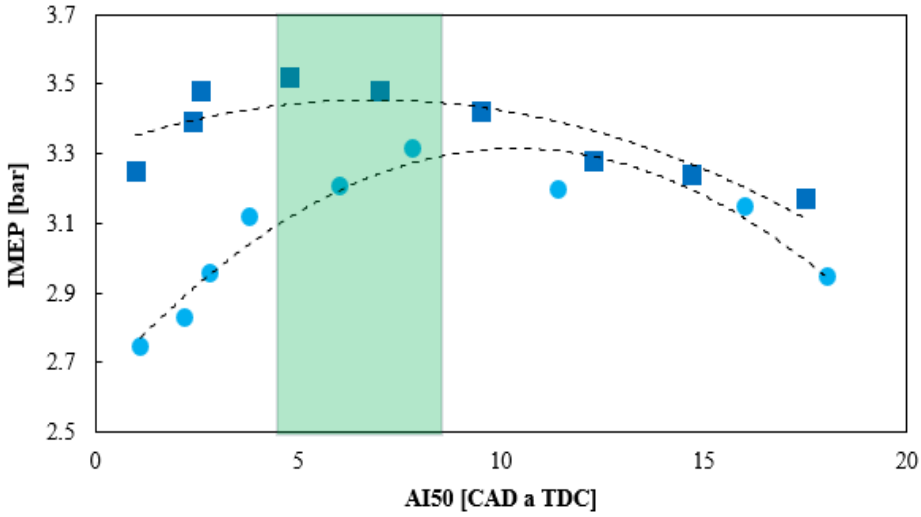

(c)

Figure 4. – (a) CoV_{IMEP} – IT, (b) IMEP – IT and (c) IMEP – AI50 in which is highlighted the MBT area of the engine in green, for the two configurations at V_d = 12.5 V and V_d = 11 V using the same t_{on} for both.

Combustion stability (Figure 4a) was evaluated by means of the Coefficient of Variance (CoV) of the Indicated Mean Effective Pressure (IMEP), namely, the ratio between IMEP standard deviation and IMEP mean value. Figure 4a depicts the CoV values found for each ignition timing tested. Engine operating points are defined as fully stable if the CoV_{IMEP} is lower than the 4% threshold [8]. Every tested condition has demonstrated full stability by consistently exhibiting a CoV_{IMEP} lower than 2.5%. Both configurations (i.e., V_d = 11 V, t_{on} = 2 ms and V_d = 12.5 V, t_{on} = 2 ms) exhibit a similar IMEP trend in response to changes in ignition timing (Figure 4b). Specifically, the configuration at 12.5 V demonstrates a higher IMEP value compared to the 11 V case, attributed to the effects on the combustion process associated with the greater ignition energy released into the medium [32]. For instance, when considering the ignition timing that optimizes performance, i.e., -7 CAD aTDC for 11 V and -11 CAD aTDC for 12.5 V, the latter configuration is capable of increasing power output by approximately 6%. Simultaneously, a comparison between the optimized point of the 12.5 V case and the 11 V operating point at the same ignition timing indicates a reduction in delivered IMEP of about 11% for the latter. In other words, if considering the interval between -1 and -7 CAD aTDC the two settings perform about the same in terms of delivered work. However, as the ignition timing advances, the 12.5 V configuration has the ability to enhance the IMEP trend compared to the 11 V configuration, as indicated by the blue arrows in Figure 4b.

This result confirms that the increased ignition energy released by the 12.5 V configuration enables the acceleration of the flame front propagation, as depicted in Figure 4c, where IMEP is

Preprints.org (www.preprints.org) | NOT PEER-REVIEWED | Posted: 4 March 2024 doi:10.20944/preprints202403.0144.v1

displayed against AI50. AI50 is defined as the crank angle degree after the Top Dead Center (TDC) at which 50% of the fuel mass is burned (determined through the indicating analysis system, starting from the in-cylinder pressure signals, as outlined in Section 2.2). The 12.5 V setup consistently moves the IMEP curve of the 11 V configuration to lower AI50 values. To put it differently, the peak of the "umbrella" trend in the 12.5 V scenario shifts towards lower AI50 values. It is essential to note that the 12.5 V configuration facilitates the utilization of engine characteristics within the MBT area (highlighted in green in Figure 4c) to optimize performance in terms of IMEP. Furthermore, it is worth highlithing that each operating point tested in this λ condition submit a CoV_{IMEP} lower than 2.5% for both configurations, thus ensuring stable combustion.

Based on these results, the subsequent analyses will refer to the 12.5 V configuration.

3.2. Analysis of the BDI's Performance at λ = 1.6 in H_2 and Conventional Gasoline E5

Figure 5 shows the comparison between the performance obtained by using gasoline E5 and hydrogen H_2 both ignited by BDI. Both configurations present IT for MBT. As can be observed, the operating point with H_2 characterized by IT = -11 CAD aTDC can deliver approximately 3.52 bar of IMEP (Table 2). Such a value corresponds to approximately 400 J/cycle, as indicated by the integral of the heat release rate in Figure 5 (blue curves). When compared to E5 application at the same λ value, this value is about 0.97 bar lower than the one achieved through gasoline fuel, which was found to be equals to 4.49 bar. Such a value corresponds to approximately 500 J/cycle, as indicated by the integral of the heat release rate in Figure 5 (black curves).

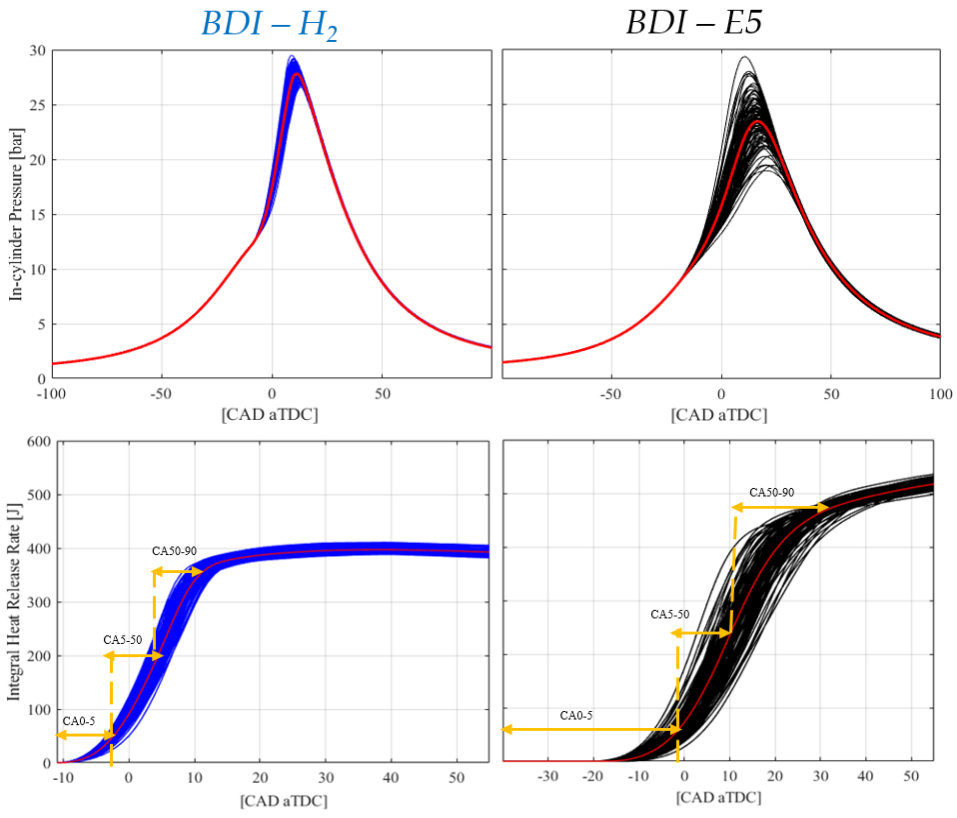

Figure 5. In-cylinder pressure traces and IHRR for both H_2 (blue curve) and E5 (black curve). The red curve of each graph indicates the average value of the 103 combustion cycles.

Table 2. main features of the operating points involving the usage of traditional spark.

Features	H_2	E5
IT [CAD aTDC]	-11	-38
CoV_{IMEP} [%]	1.56	2.8

 doi:10.20944/preprints202403.0144.v1

IMEP [bar]	3.52	4.49
AI05 [CAD aTDC]	-1.2	-2.7
AI50 [CAD aTDC]	7.1	10
AI90 [CAD aTDC]	13.8	31.5

Figure 5 reports, at optimized λ = 1.6, the in-cylinder pressure traces of H_2 with blue curves alongside those of E5, depicted in black.

In comparison to H_2, E5 displays pressure curves marked by a higher CoV_{IMEP} (2.8%), suggesting a tendency towards unstable operating conditions. Given the optimized IT for both scenarios, it's important to note that hydrogen demands much smaller IT values (-11 CAD aTDC) compared to gasoline (-38 CAD aTDC). The need for reduced ignition timing with H_2 compared to E5 is related to the combustion characteristics and properties of the respective fuels [40]. For example, the elevated flame speed of hydrogen results in quicker ignition and flame spread [23]. Additionally, the broader flammability range, combined with low ignition energy, facilitates the easy ignition of H_2 across a wide spectrum of air-fuel ratios [23].

These factors collectively impact the flame speed of hydrogen H_2 and the achievable delivered power. The lower IMEP value obtained with H_2 is related to the lower energy content per unit volume compared to gasoline, because of the reduced volumetric efficiency of the H_2-PFI operation mode.

Despite its higher energy content per unit mass, the lower density of hydrogen, when injected in the intake port, results in a reduced total energy (cf. Integral of Heat Release Rate), impacting the overall power output [41]. Table 2 summarizes the main features of the compared operating points.

3.3. Comparison between Traditional Spark and BDI at the Same IT in H_2

At the same λ=1.6, Figure 6 reports the in-cylinder and intake port pressure traces record-ed with H2 when ignited by traditional spark (green curves) and BDI (blue curves). Same IT was utilized for both igniters with BDI presenting the optimized configuration of V_d = 12.5 V and t_{on} = 2 ms. By using the same input conditions, i.e., same IT (equals to -11 CAD aTDC), BDI is able to advance the combustion process up to about 3 CAD (Figure 6a,c) thanks to the low-temperature plasma and volumetric discharge effect, as expected [38]. The acceleration of the flame front plays a crucial role in extending the lean stable limit of the engine [35]. Under these operating conditions, BDI demonstrates its potential application for higher λ values, aiming to extend the lean stable limit compared to conventional spark ignition. Furthermore, the low engine speed and load conditions, as those set in the experimental tests, together with the lean air-fuel ratio, and the short duration of the tests, prevent the attainment of high temperatures. Consequently, backfires remain few and may go un-detected by the cylinder pressure sensor. However, it is evident that the intake pressure can exhibit spikes detected by the sensor when the conventional spark ignition system is used; a pattern never observed in case of BDI. In Figure 6b is underscored the phenomenon of back-fire attributable to spark utilization. Such a behavior could be related to enhanced combustion efficiency with BDI, which reduces the presence of unburned H_2 that might re-enter the intake during valve overlap and aspiration phase. Considering the earlier discussion on operating temperature and pressure, the conditions where no backfire event occurred may be linked to the igniter characteristics. Considering the results obtained so far, additional operating points with the conventional spark were not explored further. Instead, optimization efforts were directed towards the BDI system, focusing on exploring and optimizing ignition timings at two others distinct λ values, specifically λ = 2.0 and λ = 2.3 (section 3.4).

Preprints.org (www.preprints.org) | NOT PEER-REVIEWED | Posted: 4 March 2024 doi:10.20944/preprints202403.0144.v1

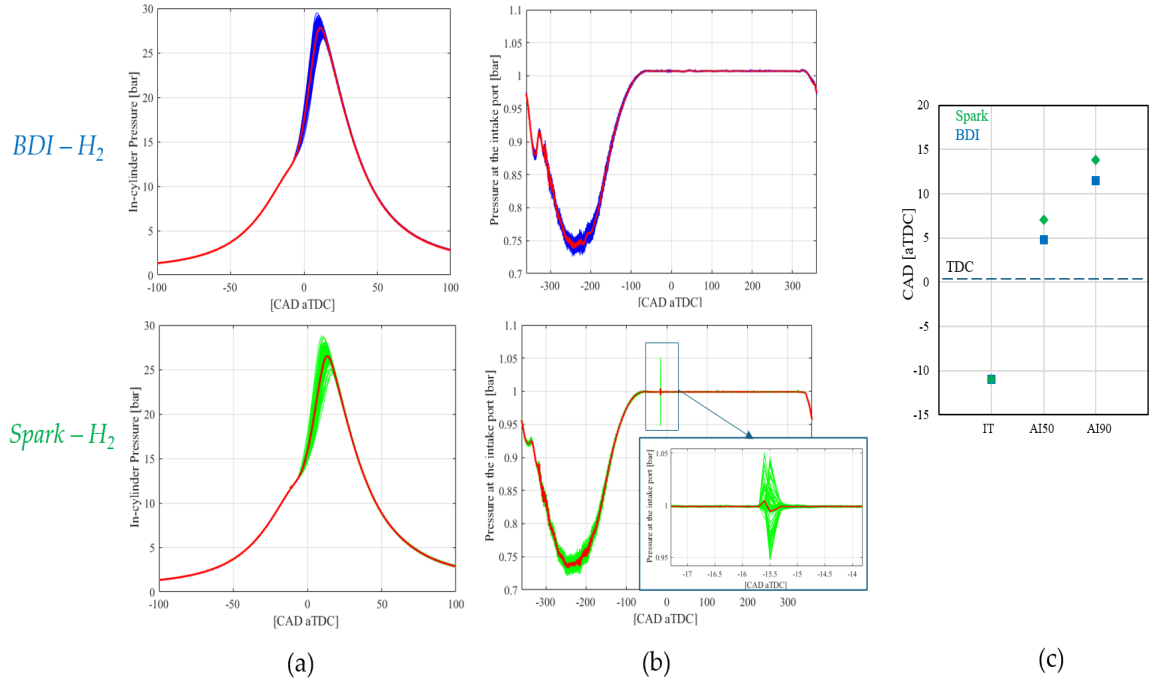

Figure 6. (a) in-cylinder pressure traces, (b) pressure at the intake port traces and (c) flame front propagation for BDI and Traditional Spark using H_2.

3.4. Extension of the BDI Lean Operating Condition

Figure 7 illustrates the optimization of performance through IT adjustment at three distinct λ values examined in this study. With the aim of ensuring optimal performance, the IT has to be advanced by moving towards leaner conditions because of the combustion duration increase (Figure 7a) [36]. The maximum in-cylinder pressure (Figure 8) and IMEP tend to decrease as the mixture is leaned, attributed to the diminished amount of fuel injected into the chamber [36]. For each λ tested, the MBT is obtained with the AI50 around 4-7 CAD aTDC (values reported in Figure 7a,b), as previously showed in Figure 4. Furthermore, differently from other fuels previously tested on the same engine [36,38], the rise in CoV_{IMEP} (Figure 7c) is not as pronounced when leaning the mixture. This phenomenon is likely attributed to the broader flammability and stability range of hydrogen across a wider lambda range [13]. For the sake of completeness, Figure 8 displays the in-cylinder pressure traces at each λ analyzed and the corresponding integral of heat release rate (IHRR).

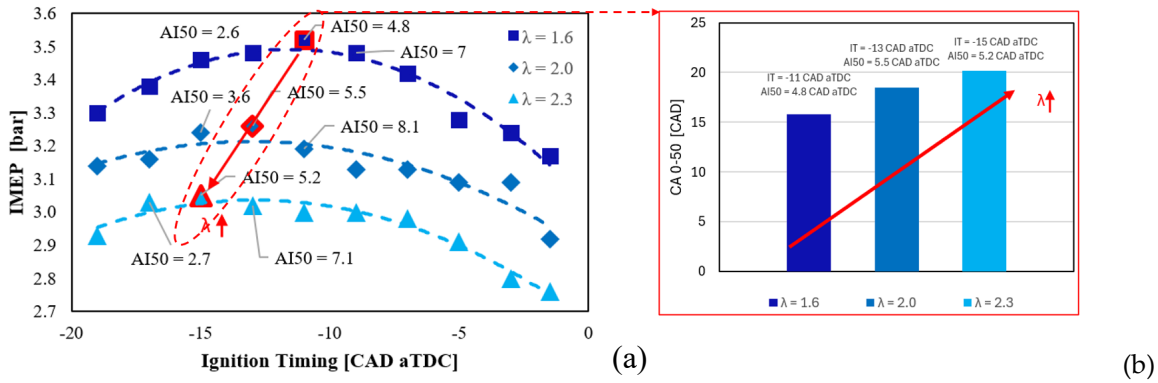

 doi:10.20944/preprints202403.0144.v1

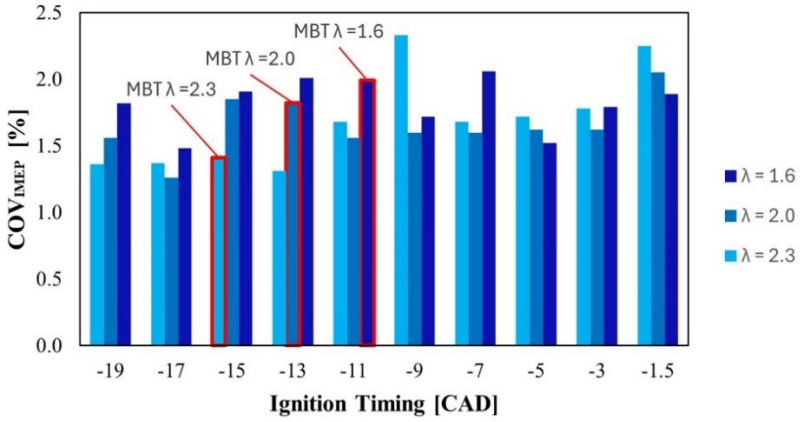

(c)

Figure 7. (a) IMEP, (b) CA 0-50 and (c) CoV_{IMEP} for the three values of λ analyzed (λ = 1.6, λ = 2.0 and λ = 2.3) in which the operating points falling within the MBT area at a specific IT, dependent on the λ value, are underlined in red.

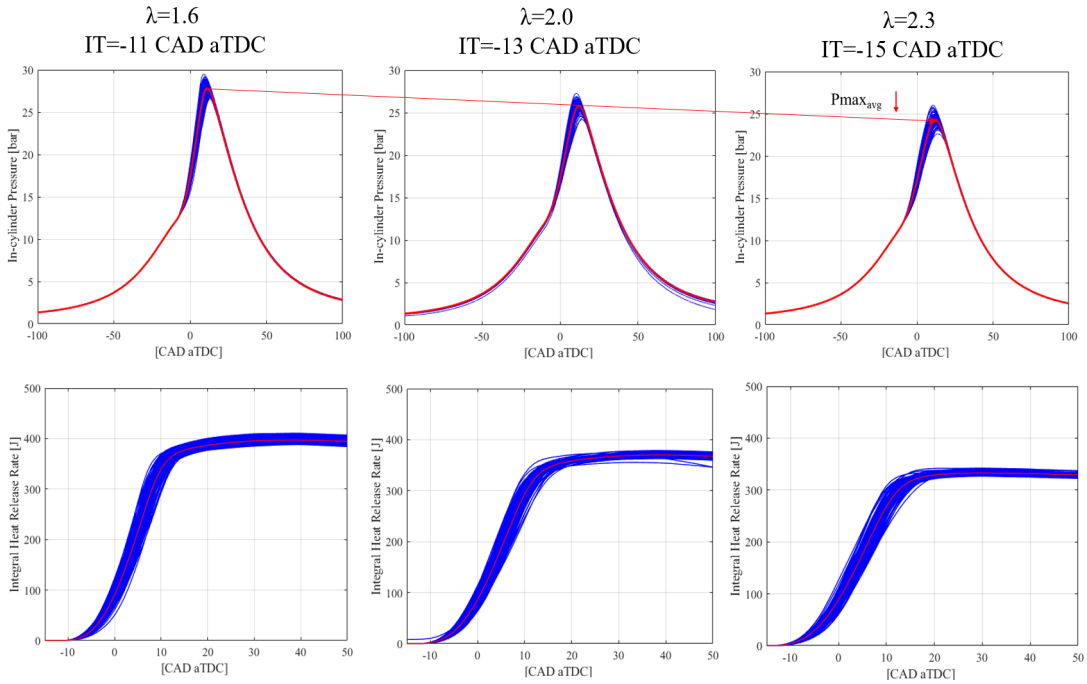

Figure 8. In-cylinder pressure traces and IHRR for the three values of λ analyzed (λ = 1.6, λ = 2.0 and λ = 2.3) and corresponding IT.

4. Conclusions

In conclusion, the investigation focused on the optimization of ACIS gen2-BDI system performance at λ = 1.6, considering both hydrogen (H_2) and conventional gasoline E5 fuels. The study examined control parameters, combustion stability, and in-cylinder pressure traces to assess the system effectiveness. At λ = 1.6, the BDI system demonstrated consistent stability across various ignition timings and driving voltages. The configuration with a higher driving voltage (12.5 V) exhibited enhanced performance, indicating the potential for increased power output. The results highlighted the BDI system ability to accelerate flame front propagation, as evidenced by the shift in the in-cylinder pressure curves and the improvement in stability at optimized ignition timings. Comparing hydrogen and gasoline E5 at λ = 1.6, hydrogen-PFI showed a lower IMEP but better combustion stability with a lower CoV_{IMEP}. The shorter ignition timing requirement for hydrogen was attributed to its combustion characteristics, including higher flame speed and broader flammability

 doi:10.20944/preprints202403.0144.v1

range. Additionally, comparing the BDI and traditional spark ignition systems at the same ignition timing for hydrogen, the BDI system demonstrated the capability to advance the combustion process, extending the lean stable limit. The absence of backfire events in the BDI system is attributed to less energy residual stored into the coil and to enhanced combustion efficiency, further emphasized its potential for leaner operating conditions. Investigations were also extended to leaner conditions (λ = 2.0 and λ = 2.3), emphasizing the need for advanced ignition timing to optimize combustion timing and therefore power output. Despite a decrease in maximum in-cylinder pressure and IMEP as the mixture leaned, the BDI system exhibited stability, and the reduction in CoV_{IMEP} was less pronounced, showcasing hydrogen broader flammability range. In summary, the BDI system, particularly with a driving voltage of 12.5 V, demonstrated promising capabilities in enhancing combustion characteristics and stability, emphasizing its potential for efficient and stable operation in lean conditions with hydrogen fuel.

Author Contributions: Conceptualization, F.R. and M.B.; methodology, F.R., M.A. and S.P; software, F.R. and M.A.; validation, S.P. and M.B.; formal analysis, J.Z. and S.P.; investigation, F.R., M.A. and S.P.; data curation, F.R., M.A. and S.P.; writing—original draft preparation, F.R.; writing—review and editing, F.R., J.Z. and M.B.; visualization, F.R. and M.A.; supervision, C.N.G. and M.B.; project administration, C.N.G. and M.B.; funding acquisition, M.B.. All authors have read and agreed to the published version of the manuscript.

Funding: The research has been partially funded by Ministero dell'Istruzione, dell'Università e della Ricerca (MIUR), Italy, through the PRIN 2020 funding source, project H2ICE, grant number 2020R92Y3Z, and by the University of Perugia grant "Fondo Ricerca di Ateneo, edizione 2021". The igniters used for the research have been provided by Federal Mogul Powertrain Italy, a Tenneco Group Company.

Data Availability Statement: Dataset available on request from the authors.

Conflicts of Interest: The authors declare no conflict of interest.

Nomenclature

aBDC	after Bottom Dead Center
ACIS	Advanced Corona Ignition System
AI05	Crank angle degree after the Top Dead Center (TDC) for which 5% of the mass is burned
AI50	Crank angle degree after the Top Dead Center (TDC) for which 50% of the mass is burned
AI90	Crank angle degree after the Top Dead Center (TDC) for which 90% of the mass is burned
aTDC	after Top Dead Center
BDI	Barrier Discharge Igniter
CA 0-50	Crank angle degree from IT to AI05
CA 5-50	Crank angle degree from AI05 to AI50
CA 50-90	Crank angle degree from AI50 to AI90
CAD	Crank Angle Degree
CO	Carbon Monoxide
CoV_{IMEP}	Coefficient of Variance of IMEP
DI	Direct Injection
D/GPF	High-efficiency Particulate Filters
E5	Gasoline
E85	Ethanol
ECU	Engine Control Unit
EGR	Exhaust Gas Recirculation
H_2	Hydrogen
HC	Hydrocarbons
ICE	Internal Combustion Engine
IHRR	Integral Heat Release Rate
IMEP	Indicated Mean Effective Pressure
IT	Ignition Timing
λ	Relative Air-Fuel ratio
LTC	Low-Temperature Combustion
LTP	Low-Temperature Plasma
MBT	Maximum Brake Torque

 doi:10.20944/preprints202403.0144.v1

NO_x	Nitrogen Oxides
O_2	Oxygen
PFI	Port Fuel Injection
SCR	Selective Catalytic Reducers
SI	Spark Ignition
t_{on}	Activation Time
V_d	Driving Voltage

References

1. D. Suresh, and E. Porpatham. "Influence of high compression ratio and hydrogen addition on the performance and emissions of a lean burn spark ignition engine fueled by ethanol-gasoline." International Journal of Hydrogen Energy 48.38 (2023): 14433-14448. Doi: 10.1016/j.ijhydene.2022.12.275
2. R.D. Reitz, H. Ogawa, R. Payri, et al. "IJER editorial: the future of the internal combustion engine." Int. J. Engine Res. 21 (1) (2020) 3–10. Doi: 10.1177/1468087419877990
3. D. Xiongbo, et al. "Performance analysis and comparison of the spark ignition engine fuelled with industrial by-product hydrogen and gasoline." Journal of Cleaner Production 424 (2023): 138899. Doi: 10.1016/j.jclepro.2023.138899
4. J. Dernotte, P. M. Najt, and R. P. Durrett. "Downsized-Boosted Gasoline Engine with Exhaust Compound and Dilute Advanced Combustion." SAE International Journal of Advances and Current Practices in Mobility 2.2020-01-0795 (2020): 2665-2680. Doi: 10.4271/2020-01-0795
5. J. Zembi, et al. "Numerical investigation of water injection effects on flame wrinkling and combustion development in a GDI spark ignition optical engine." SAE Technical Paper, 2021, 2021-01-0465. Doi: 10.4271/2021-01-0465
6. J. Zembi, et al. "Investigations on the impact of port water injection on soot formation in a DISI engine through CFD simulations and optical methods." Fuel, 2023, 337, 127170. Doi: 10.1016/j.fuel.2022.127170
7. S. R. Dadam, et al. "Diagnostic evaluation of exhaust gas recirculation (EGR) system on gasoline electric hybrid vehicle. " SAE Technical Paper, 2020, 2020-01-0902. Doi: 10.4271/2020-01-0902
8. F. Ricci, et al. "Comparative analysis of thermal and non-thermal discharge modes on ultra-lean mixtures in an optically accessible engine equipped with a corona ignition system." Combustion and Flame 259 (2024): 113123. Doi: 10.1016/j.combustflame.2023.113123
9. A. P. Singh, V. Kumar, and A. K.Agarwal. "Evaluation of comparative engine combustion, performance and emission characteristics of low temperature combustion (PCCI and RCCI) modes." Applied Energy 278 (2020): 115644. Doi: 10.1016/j.apenergy.2020.115644
10. J. Pielecha, K. Skobiej, and K. Kurtyka. "Exhaust emissions and energy consumption analysis of conventional, hybrid, and electric vehicles in real driving cycles." Energies 13.23 (2020): 6423. Doi: 10.3390/en13236423
11. O. C. Anika, et al. "Prospects of low and zero-carbon renewable fuels in 1.5-degree net zero emission actualisation by 2050: A critical review." Carbon Capture Science & Technology 5 (2022): 100072. Doi: 10.1016/j.ccst.2022.100072
12. F. Campos-Carriedo, et al. "How can the European Ecodesign Directive guide the deployment of hydrogen-related products for mobility?" Sustainable Energy & Fuels 7.6 (2023): 1382-1394. Doi: 10.1039/D2SE01486F
13. P. Sementa, et al. "Exploring the potentials of lean-burn hydrogen SI engine compared to methane operation." International Journal of Hydrogen Energy 47.59 (2022): 25044-25056. Doi: 10.1016/j.ijhydene.2022.05.250
14. Q-h Luo , B-g Sun. "Inducing factors and frequency of combustion knock in hydrogen internal combustion engines." IJHE 2016;41(36):16296–305. Doi: 10.1016/j.ijhydene.2016.05.257
15. K. Aydin, R. Kutanoglu. "Effects of hydrogenation of fossil fuels with hydrogen and hydroxy gas on performance and emissions of internal combustion engines." IJHE 2018;43(30):14047–58. Doi: 10.1016/j.ijhydene.2018.04.026
16. C. B. Srinivasan, R. Subramanian. "Hydrogen as a Spark Ignition Engine Fuel Technical Review." Int. J. Mech. Mechatron. Eng. IJMME-IJENS 2014, 14, 111–117.
17. M.A. Ceviz, I. Kaymaz. "Temperature and air–fuel ratio dependent specific heat ratio functions for lean burned and unburned mixture." Energy Convers. Manag. 2005, 46, 2387–2404. Doi: 10.1016/j.enconman.2004.12.009
18. S. Verhelst, R. Sierens, S. Verstraeten. "A Critical Review of Experimental Research on Hydrogen Fueled SI Engines." SAE Trans.2006, 115, 264–274. Doi: 10.4271/2006-01-0430.
19. C. Shi, C. Ji, S. Wang, et al. "Experimental and numerical study of combustion and emissions performance in a hydrogen-enriched Wankel engine at stoichiometric and lean operations." Fuel 2021;291:120181. Doi: 10.1016/j.fuel.2021.120181

20. P. Dimitriou, M. Kumar, T. Tsujimura, et al. "Combustion and emission characteristics of a hydrogen-diesel dual-fuel engine." IJHE 2018;43(29): 13605–17. Doi: 10.1016/j.ijhydene.2018.05.062
21. H. Wu, X. Yu, Y. Du, et al. "Study on cold start characteristics of dual fuel SI engine with hydrogen direct-injection." Appl Therm Eng 2016;100: 829–39. Doi: 10.1016/j.applthermaleng.2016.02.097
22. H. Serin, S¸. Yıldızhan. "Hydrogen addition to tea seed oil biodiesel: Performance and emission characteristics." IJHE 2018;43(38):18020–7. Doi: 10.1016/j.ijhydene.2017.12.085
23. J. Gao, et al. "Review of the backfire occurrences and control strategies for port hydrogen injection internal combustion engines." Fuel 307 (2022): 121553. Doi: 10.1016/j.fuel.2021.121553
24. H. T. Cong, J. K. Kang, K. C. Noh, et al. "Controlling backfire using changes of the valve overlap period for a hydrogen-fueled engine using an external mixture." Internal Combustion Engine Division Fall Technical Conference. 48116. 2007: 243–51. Doi: 10.1115/ICEF2007-1702
25. Garmsiri S. "Study of an internal combustion engine to burn hydrogen fuel and backfire elimination using a carburetor fuel delivery method." UOIT 2010.
26. Y. Ye, W. Gao, Y. Li, et al. "Numerical study of the effect of injection timing on the knock combustion in a direct-injection hydrogen engine." IJHE 2020;45(51):27904–19. Doi: 10.1016/j.ijhydene.2020.07.117
27. L. Ceschini, A. Morri, E. Balducci, et al. "Experimental observations of engine piston damage induced by knocking combustion." Materials Design 2017;114:312–25. Doi: 10.1016/j.matdes.2016.11.015
28. P. M. Dieguez, J. Urroz, D. Sainz, et al. "Characterization of combustion anomalies in a hydrogen-fueled 1.4 L commercial spark-ignition engine by means of in-cylinder pressure, block-engine vibration, and acoustic measurements." Energy Convers Manage 2018;172:67–80. Doi: 10.1016/j.enconman.2018.06.115
29. T. Tsujimura, Y. Suzuki. "The utilization of hydrogen in hydrogen/diesel dual fuel engine." IJHE 2017;42(19):14019–29. Doi: 10.1016/j.ijhydene.2017.01.152
30. S. Falfari, et al. "Hydrogen Application as a Fuel in Internal Combustion Engines." Energies 16.6 (2023): 2545. Doi: 10.3390/en16062545
31. J. Zembi, et al. "Numerical Simulation of the Early Flame Development Produced by a Barrier Discharge Igniter in an Optical Access Engine." SAE Technical Paper, 2021, 2021-24-0011. Doi: 10.4271/2021-24-0011
32. F. Ricci, et al. "Luminosity and thermal energy measurement and comparison of a dielectric barrier discharge in an optical pressure-based calorimeter at engine relevant conditions." SAE Technical Paper, 2021, 2021-01-0427. Doi: 10.4271/2021-01-0427
33. S. M. Starikovskaia. "Plasma assisted ignition and combustion. " J Phys D Appl Phys 2006;39 (16):R265–99. Doi: 10.1088/0022-3727/39/16/r01
34. J. Zembi, et al. "Modeling of thermal and kinetic processes in non-equilibrium plasma ignition applied to a lean combustion engine." Applied Thermal Engineering, 2021, 197, 117377. Doi: 10.1016/j.applthermaleng.2021.117377
35. C. A. Idicheria, P. M. Najt. "Potential of advanced corona ignition system (ACIS) for future engine applications." In: Ignition Syst. Gasol. Engines. Cham: Springer International Publishing; 2017. p. 315–31. Doi: 10.1007/978-3-319-45504-4_19
36. R. Martinelli, et al. "Lean Combustion Analysis of a Plasma-Assisted Ignition System in a Single Cylinder Engine fueled with E85." SAE Technical Paper, 2022, 2022-24-0034. Doi: 10.4271/2022-24-0034
37. F. Ricci, et al. "Energy characterization of an innovative non-equilibrium plasma ignition system based on the dielectric barrier discharge via pressure-rise calorimetry." Energy Conversion and Management 244 (2021): 114458. Doi: 10.1016/j.enconman.2021.114458
38. V. Cruccolini, et al. "Comparative analysis between a barrier discharge igniter and a streamer-type radio-frequency corona igniter in an optically accessible engine in lean operating conditions." SAE Technical Paper, 2020, 2020-01-0276. Doi: 10.4271/2020-01-0276
39. N. Azeem, et al. "Comparative Analysis of Different Methodologies to Calculate Lambda (λ) Based on Extensive And systemic Experimentation on a Hydrogen Internal Combustion Engine." SAE Technical Paper, 2023, 2023-01-0340. Doi: 10.4271/2023-01-0340
40. L. Wanget al. "The effect of hydrogen injection parameters on the quality of hydrogen–air mixture formation for a PFI hydrogen internal combustion engine." International Journal of Hydrogen Energy 42.37 (2017): 23832-23845. Doi: 10.1016/j.ijhydene.2017.04.086
41. B. J. Shinde, and K. Karunamurthy. "Recent progress in hydrogen fuelled internal combustion engine (H2ICE)–A comprehensive outlook." Materials Today: Proceedings 51 (2022): 1568-1579. Doi: 10.1016/j.matpr.2021.10.378